

# Synthesis, Isolation, Structure Elucidation, and Color Properties of 10-Acetyl-pyranoanthocyanins

Sergio Gómez-Alonso,<sup>†,‡</sup> Dora Blanco-Vega,<sup>§</sup> M. Victoria Gómez,<sup>‡,||</sup> and Isidro Hermosín-Gutiérrez<sup>\*,†,§</sup>

<sup>†</sup>Instituto Regional de Investigación Científica Aplicada, Universidad de Castilla-La Mancha, Campus Universitario s/n, 13071 Ciudad Real, Spain

<sup>‡</sup>Fundación Parque Científico y Tecnológico de Albacete, Paseo de la Innovación, 1, 02006, Albacete, Spain

<sup>§</sup>Escuela de Ingenieros Agrónomos de Ciudad Real, Universidad de Castilla-La Mancha, Ronda de Calatrava 7, 13071 Ciudad Real, Spain

<sup>||</sup>Instituto Regional de Investigación Científica Aplicada, Dpto. Química Orgánica, Inorgánica y Bioquímica, Universidad de Castilla-La Mancha, Campus Universitario s/n, 13071 Ciudad Real, Spain

## Supporting Information

**ABSTRACT:** Grape anthocyanins reacted with diacetyl, a secondary metabolite of microorganisms involved in winemaking, to form 10-acetyl-pyranoanthocyanins, a type of anthocyanin-derived pigment similar to other vitisin-type pyranoanthocyanins found in red wines. The structures of 10-acetyl-pyranomalvidin-3- $\beta$ -*O*-glucoside and 10-acetyl-pyranopeonidin-3- $\beta$ -*O*-glucoside were confirmed by spectroscopic methods (UV-vis, MS/MS, and NMR) after their synthesis and isolation. In contrast to other vitisin-type pyranoanthocyanins, the newly described 10-acetyl-pyranoanthocyanins exhibited differentiated color-related properties. They showed an important tendency to occur as colorless hemiacetals at C-10 under wine pH conditions, while co-occurrence of flavylium cation and quinoidal base yielded a broad visible absorbance band around 510–520 nm. Moreover, they easily reacted with bisulfite in acidic aqueous solution (pH 2.0), but the expected bleaching was not observed. Bisulfite bonded to the carbonyl of 10-acetyl substituent instead of the expected C-10 position of the pyranoanthocyanin core, thus giving rise to a red pigment hypsochromically shifted toward orangish nuances (maximum absorbances at 487–491 nm).

**KEYWORDS:** red wine, color, pyranoanthocyanins, diacetyl, LC-MS, UV-vis, NMR

## ■ INTRODUCTION

Red wine color chemistry has attracted for decades the attention of many researchers.<sup>1</sup> In addition to the early proposed formation of polymeric pigments by reaction between anthocyanins and tannins, a new class of nonpolymeric pigments have gained position in this field, namely, the so-called pyranoanthocyanins. The general pathway of pyranoanthocyanin formation involves an anthocyanin and a compound having a polarizable double bond (pyranoanthocyanin precursor) that reacts to give rise to a new pyrano ring fused to the anthocyanin molecule.<sup>2</sup> Many pyranoanthocyanin precursors have been identified, including those derived from some yeast metabolites produced during alcoholic fermentation (e.g., pyruvic acid or acetaldehyde) and also other compounds generated from grape phenolics over wine aging (e.g., free hydroxycinnamic acids or 8-vinyl-flavanols). Pyranoanthocyanins also have been found in other natural sources or their processed products.<sup>2</sup> In recent years, some pyranoanthocyanins with the simplest structures (A-type vitisins or 10-carboxy-pyranoanthocyanins and 10-methyl-pyranoanthocyanins) have been identified as the starting point for the formation of more complex pyranoanthocyanins<sup>3–8</sup> or their transformation into other kinds of nonred pigments.<sup>9,10</sup>

The contribution of pyranoanthocyanins to total red wine color has been largely suggested on the basis of their color stability in comparison to grape anthocyanins from which they derived. Several studies on aqueous solution equilibria in which

pyranoanthocyanins are involved have demonstrated that they are more resistant than anthocyanins from which they derive with regard to both the hydration of the red-colored flavylium cation (leading to the formation of colorless hemiacetal form) and the bleaching by bisulfite.<sup>5,11–17</sup> The aforementioned studies supported that almost all of the pyranoanthocyanins molecules present in wines really contribute to red wine color, as they predominantly occur at wine pH conditions as red-orange-colored flavylium cations without significant variations due to changes in pH or bisulfite addition.

In a previous study dealing with the formation of diverse pyranoanthocyanins in a model wine, we suggested the formation of a new member of this pigment family obtained from diacetyl, a secondary product of lactic acid bacteria metabolism, which was tentatively assigned as 10-acetyl-pyranoanthocyanins.<sup>18</sup> In addition, we also found evidence of the occurrence of 10-acetyl-pyranoanthocyanins in real red wine samples. To ascertain the role in red wine color of this new kind of pigment derived from grape anthocyanins and fermentation metabolites, the aim of our work was the synthesis and isolation of 10-acetyl-pyranoanthocyanins to confirm the suggested structure and also to study their chromatic

**Received:** September 7, 2012

**Revised:** November 20, 2012

**Accepted:** November 21, 2012

**Published:** November 21, 2012

characteristics under variable pH conditions and resistance to bleaching by bisulfite.

## MATERIALS AND METHODS

**Chemicals.** All solvents were of high-performance liquid chromatography (HPLC) quality, and water was of Milli-Q quality. Malvidin 3-glucoside (PhytoLab, Vestenbergsgreuth, Germany) was used as standard for quantification of anthocyanins in red grape skin extracts. Diacetyl (2,3-butanedione;  $\geq 99.0\%$ , Fluka) was the reagent used for the formation of 10-acetyl-pyranoanthocyanins from grape skin anthocyanins.

**Red Grape Skin Extracts.** Red grapes of *V. vinifera* Garnacha Tintorera variety were chosen because of its unique anthocyanin profile: similar high proportions of peonidin- and malvidin-based anthocyanins, mainly occurring as nonacylated derivatives. Batches of 100 g of healthy red grapes were collected at technological maturity and finger pressed to remove the pulp and the seeds. The remaining skins were washed in water ( $3 \times 25$  mL) and softly dried twice by patting them between sheets of filter paper. The dried skins were extracted with 100 mL of a mixture 50:48.5:1.5 (v/v) of  $\text{CH}_3\text{OH}/\text{H}_2\text{O}/\text{HCOOH}$ ,<sup>19</sup> using a homogenizer (Heidolph DIAX 900) for 2 min and then centrifuging at 2500g at 5 °C for 15 min. The supernatant of this crude grape skin extract was stored at  $-20$  °C until use.

**Purification of Red Grape Skin Extracts.** Anthocyanins present in red grape skin extracts were isolated, to prevent interferences during the formation reaction of 10-acetyl-pyranoanthocyanins. The separation procedure was adapted from the SPE method developed for isolation of grape skin flavonols,<sup>19</sup> but this time, the interest was focused on the recovery of the retained anthocyanins by cation exchange. The crude grape skin extract (3 mL) was first dried in a rotary evaporator (35 °C), then redissolved in 0.1 N HCl (3 mL), and passed through the MCX cartridges (Waters) previously conditioned with 5 mL of methanol and 5 mL of water. After they were washed with 5 mL of 0.1 N HCl and 5 mL of water, the nonanthocyanin phenolic compounds were eluted with  $3 \times 5$  mL of methanol. Fixed anthocyanins were removed using  $3 \times 5$  mL of 2% (w/v) ammonia in methanol–water (80:20 v/v), and the cationic exchanger material was regenerated with  $3 \times 5$  mL of 2% (w/v) hydrochloric acid in methanol–water (80:20 v/v). The anthocyanin eluate (deep blue color solution) was immediately acidified by adding 4 N HCl until an intense red color was regenerated. After they were dried in a rotary evaporator (35 °C), anthocyanins were solved in acetone (5 mL), and an excess of ammonium chloride was eliminated by filtration. A further purification by solid-phase extraction (SPE) on C18 cartridges (Sep Pack, Merck) was necessary to completely remove the salts: after acetone was removed in a rotary evaporator (35 °C), the residue was redissolved in 0.1 N HCl and applied to a SPE cartridge, previously conditioned with 5 mL of methanol and 5 mL of water; the purified anthocyanins were recovered with 2% HCl in methanol and stored at  $-20$  °C until use.

**Reaction of Formation of 10-Acetyl-pyranoanthocyanins.** Reaction conditions described for the synthesis of 10-carboxy-pyranomalvidin-3-glucoside<sup>12</sup> were adapted for improving reaction yield. The adequate volume of purified grape skin extract that contained 100 mg of total anthocyanins (as malvidin-3-glucoside equivalents) was dried in a rotary evaporator (35 °C). The solid residue was dissolved in water (50 mL) in an amber glass bottle (60 mL), and the pH was adjusted to 2.5 with 1 N HCl. Further addition of diacetyl (9.85 mL) was made to obtain a molar ratio diacetyl:anthocyanin of 500:1 with regard to the total anthocyanin concentration (2000 mg/L of mv-3-glc equivalents). After the bottle was closed, the reaction mixture was gently blended and allowed to react in an oven at 35 °C. The reaction was stopped after maximum chromatographic yield was reached (usually 17–18 h) by cooling and removing the excess of diacetyl. Thus, the reaction mixture was applied to a chromatographic glass column (2.5 cm  $\times$  30 cm) filled with Amberlite XAD-7 (2 h methanolic suspension, followed by filling of the column and rinsing with  $2 \times 125$  mL water). The first wash with

methanol–water (25:75 v/v) removed excess diacetyl (yellow eluate) and nonreacted anthocyanins (orange eluate). Further elution with methanol–water (40:60 v/v) yielded a fraction containing the expected reaction products (red-purple eluate) that were submitted to countercurrent chromatography in the next step.

**Fractionation of Main Reaction Products by Fast Centrifugal Partition Chromatography (FCPC).** Countercurrent chromatography was carried out using a FCPC system model FCPC-200 (Kromatron, France) with a total rotor volume of 198 mL and 840 partition cells. The FCPC system was connected to a semipreparative ternary pump model BETA-50 (ECOM, Czech Republic), a UV–vis detector model Flash 06S DAD 600 (ECOM, Czech Republic), and a fraction collector model CHF122SC (Advantec, United States). Samples were manually injected from a 10 mL loop through a 3725i Rheodyne valve (United States).

Separation was carried out using a gradient of a ternary biphasic solvent system composed of ethyl acetate, 1-butanol, and water and operating the FCPC system in ascending mode, at a flow rate of 5 mL/min and a rotor speed of 1750 rpm, as modified from Renault et al.<sup>20</sup> Phases composition was as follows: stationary phase, ethyl acetate–1-butanol–water (4:5:91 v/v); mobile phase A, ethyl acetate–1-butanol–water (77:15:8 v/v); and mobile phase B, ethyl acetate–1-butanol–water (40:46:14 v/v). Each phase was acidified with 0.1% trifluoroacetic acid. The sample was injected dissolved in 10 mL of a mixture of stationary phase and mobile phase A (50:50 v/v). The linear gradient was as follows: 0 min, 100% mobile phase A; 90 min, 100% mobile phase B; and 115 min, 100% mobile phase B. Fractions of 10 mL were collected every 2 min from minute 12. Detection was performed at 280 and 520 nm.

The composition of the fractions was determined using HPLC–diode array detection–electrospray ionization mass spectrometry (DAD-ESI-MS/MS), and those containing the compounds of interest were stored at  $-20$  °C until further purification. Two main fractions were collected containing the main produced 10-acetyl-pyranoanthocyanins derived from the main anthocyanins present in grape skin extracts, namely, the 3-glucosides of malvidin and peonidin.

**Semipreparative HPLC Purification of Main Produced 10-Acetyl-pyranoanthocyanins.** FCPC fractions enriched in 10-acetyl-pyranoanthocyanins were purified using a semipreparative HPLC system composed of two HPLC pumps model 510, a gradient controller model 600, a manual injector model U6K, and an UV–vis detector model PDA-996 all from Waters (United States) and controlled by the Millennium v. 3.2 software (Waters). The volume injection was 250  $\mu\text{L}$ , and separation was carried out in a Kromasil C18 column (250 mm  $\times$  10 mm i.d., 5  $\mu\text{m}$ ; Análisis Vínicos, Spain), flow 2 mL/min, using a biphasic solvent gradient: phase A, water–acetonitrile–formic acid (87:3:10 v/v); phase B, water–acetonitrile–formic acid (40:50:10 v/v). The gradient was as follows: 0 min, 75% A; 8 min, 65% A; 18 min, 65% A; 21 min, 0% A; 23 min, 0% A; and 25 min, 75% A. Detection was performed at 520 nm, and fractions were manually collected. Fractions containing the purified 10-acetyl-pyranoanthocyanins were dried under vacuum, redissolved in 0.1 N HCl methanol, and dried again under vacuum to obtain the compounds as chloride salts, which were stored at  $-20$  °C until further use.

**Analytical HPLC-DAD-ESI-MS/MS.** HPLC separation, identification, and quantification of 10-acetyl-pyranoanthocyanins were performed on an Agilent 1100 Series system (Agilent, Germany), equipped with DAD (G1315B) and LC/MSD Trap VL (G2445C VL) ESI-MS/MS system and coupled to an Agilent Chem Station (version B.01.03) data-processing station. The mass spectra data were processed with the Agilent LC/MS Trap software (version 5.3). The reaction mixture samples and semipreparative HPLC fractions were directly injected after proper dilution if necessary (0.1 N HCl), whereas the FCPC fractions were previously dried in a rotary evaporator (35 °C) and redissolved in 0.1 N HCl. After filtration (0.20  $\mu\text{m}$ , polyester membrane, Chromafil PET 20/25, Macherey-Nagel, Düren, Germany), the samples were injected (10  $\mu\text{L}$ ) on a reversed-phase column Zorbax Eclipse XDB-C18 (2.1 mm  $\times$  150 mm; 3.5  $\mu\text{m}$  particle; Agilent, Germany), thermostatted at 40 °C, and protected

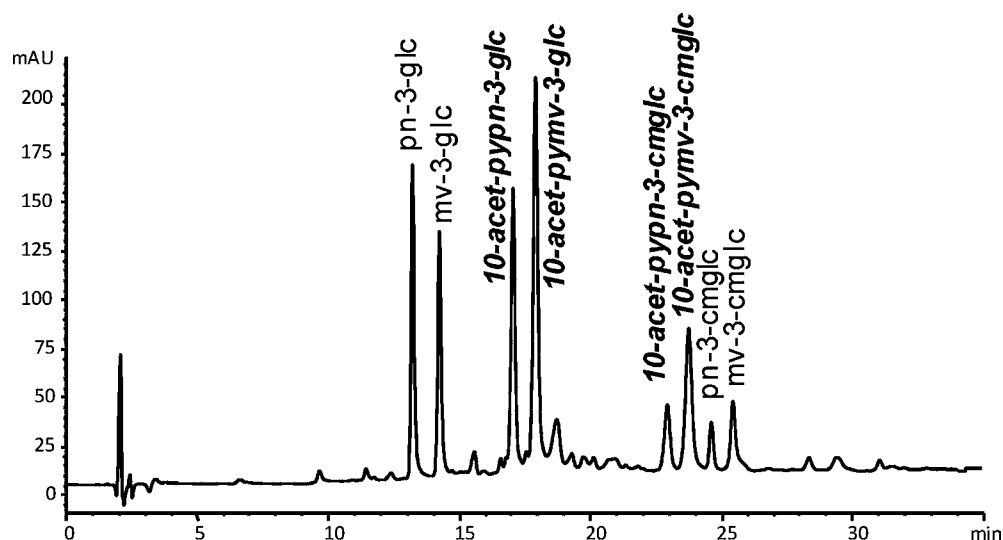


**Figure 1.** Reaction mixture after 18 h showing the formation of 10-acetyl-pyranoanthocyanins and the remaining anthocyanin precursors. Abbreviations: pn, peonidin; mv, malvidin; 3-glc, 3-glucoside; 3-cmglc, 3-(6''-*p*-coumaroyl)-glucoside; pypn, pyranopeonidin; and pymv, pyranomalvidin.

with a guard column of XDB-C8 (2.1 mm × 15 mm; 3.5 μm particle; Agilent). The chromatographic conditions were adapted from the OIV method for analysis of anthocyanins in red wines,<sup>21</sup> and the detection wavelength was 520 nm. The solvents were water/acetonitrile/formic acid (87:3:10, v/v/v, solvent A; 40:50:10, v/v/v, solvent B), and the flow rate was 0.19 mL/min. The linear gradient for solvent B was as follows: 0 min, 6%; 15 min, 30%; 30 min, 50%; 35 min, 60%; 38 min, 60%; and 46 min, 6%. For identification, ESI-MS/MS operating parameters were optimized by direct infusion of solutions of both a standard of malvidin 3-glucoside and chromatographically pure isolated 10-acetyl-pyranomalvidin-3-glucoside.

**pH Assay.** For the pH assay, solutions of each pigment (2 mM) were prepared in 12% (v/v) aqueous ethanol and added to buffer solutions with different pH values in a range between 1.0 and 13.0. The solvents used for preparation of the buffer solutions were 0.2 M KCl, 0.1 M HCl, 0.2 M HCl, 0.1 M KHC<sub>8</sub>O<sub>4</sub>H<sub>4</sub>, 0.1 M NaOH, 0.2 M NaOH, 0.1 M KH<sub>2</sub>PO<sub>4</sub>, 0.1 M tris-(hydroxymethyl)-aminomethane, 0.025 M Borax, and 0.05 M Na<sub>2</sub>HPO<sub>4</sub> according to Robinson and Stokes.<sup>22</sup> The final concentration of each pigment was 0.08 mM. All of the pigments solutions were left to equilibrate for 2 h, and then, spectroscopic absorbance curves were recorded for all of the solutions from 360 to 830 nm with a 1 nm sampling interval, using a 10 mm path length quartz cell in a Shimadzu UV-1800 spectrophotometer (Japan).

**SO<sub>2</sub> Bleaching Assay.** The bleaching by SO<sub>2</sub> was studied using the pigments solutions at pH 2.0.<sup>12</sup> To these solutions were added different aliquots of an aqueous solution of sodium bisulfite to achieve SO<sub>2</sub> concentrations in the range between 0 and 200 ppm. Spectroscopic absorbance curves were recorded for all of these solutions from 360 to 830 nm with a 1 nm sampling interval, using a 10 mm path length quartz cell in a Shimadzu UV-1800 spectrophotometer (Japan).

**Molar Extinction Coefficients and CIELAB Color Measurements.** Molar extinction coefficients of the isolated 10-acetyl-pyranoanthocyanins according to the Beer–Lambert law were determined using solutions of the pigments in the concentration range 0.01–0.16 mM at pH 1.0 and pH 3.6 buffers prepared according to Robinson and Stokes.<sup>22</sup> Spectroscopic absorbance curves were recorded from 360 to 830 nm with a 1 nm sampling interval, using a 10 mm path length quartz cell in a Shimadzu UV-1800 spectrophotometer (Japan). Molar extinction coefficients of each pigment were calculated at two different wavelengths, namely, 520 nm and the wavelength corresponding to the maximum absorbance of each pigment. Spectroscopic curves of the 0.08 mM solutions of the pigments at pH 3.6 were used to determine the color coordinates in

the CIELAB color space using CIE D65/10° illuminant/observer conditions.<sup>23</sup> All of the color calculations were performed using a computer program developed by our group.

**Structure Elucidation by Nuclear Magnetic Resonance Spectroscopy.** The assignment of the proton (<sup>1</sup>H) and carbon (<sup>13</sup>C) peaks was done by <sup>1</sup>H NMR, <sup>1</sup>H–<sup>1</sup>H correlation spectroscopy (COSY), <sup>1</sup>H–<sup>1</sup>H nuclear Overhauser effect spectroscopy (NOESY), <sup>1</sup>H–<sup>13</sup>C heteronuclear multiple-quantum correlation (HMQC), and <sup>1</sup>H–<sup>13</sup>C heteronuclear multiple bond correlation (HMBC) experiments in CD<sub>3</sub>OD and DMSO-*d*<sub>6</sub> containing different proportions of CF<sub>3</sub>COOD (from 2 to 30%). The NMR experiments were carried out using a Varian Inova NMR spectrometer operating at 499.772 MHz for <sup>1</sup>H and at 125.678 MHz for <sup>13</sup>C. The spectrometer was equipped with a gradient amplifier and a four-nucleus 5 mm <sup>1</sup>H{<sup>15</sup>N–<sup>31</sup>P}PFG high-field indirect detection probe. All 1D and 2D experiments (COSY, NOESY, HMQC, and HMBC) were performed at 298 K using standard pulse sequences from the Varian library.

## RESULTS AND DISCUSSION

**Synthesis and Isolation of the 10-Acetyl-pyranoanthocyanins Derivatives Formed from the 3-Glucosides of Peonidin and Malvidin.** Starting from the most common reaction conditions found in the literature about the synthesis of pyranoanthocyanins from their anthocyanin precursors,<sup>12</sup> we assayed different conditions to increase yield reaction and minimize anthocyanin thermal degradation and also product degradation following an extended reaction time. We finally found that use of a high anthocyanin concentration (2000 mg/L) with a great excess of diacetyl (molar ratio 500:1 with regard to anthocyanins) during a relatively short reaction time (18 h) led to the best results in aqueous solution at pH 2.5 and 35 °C.

The used red grape skin extract contained two main nonacylated anthocyanins in similar proportions, namely, the 3-glucosides of peonidin and malvidin (pn-3-glc and mv-3-glc, respectively), together with little amounts of their respective 6''-*p*-coumaroylated derivatives (Figure 1). When the reaction was stopped, less than 10–19% of initial individual anthocyanins still remained, and the expected 10-acetyl-pyranoanthocyanins were observed, but their yields were far from quantitative: on the basis of calibration curves obtained for pn-3-glc and mv-3-glc and their isolated reaction products (the purity of isolated compounds was checked by HPLC peaks

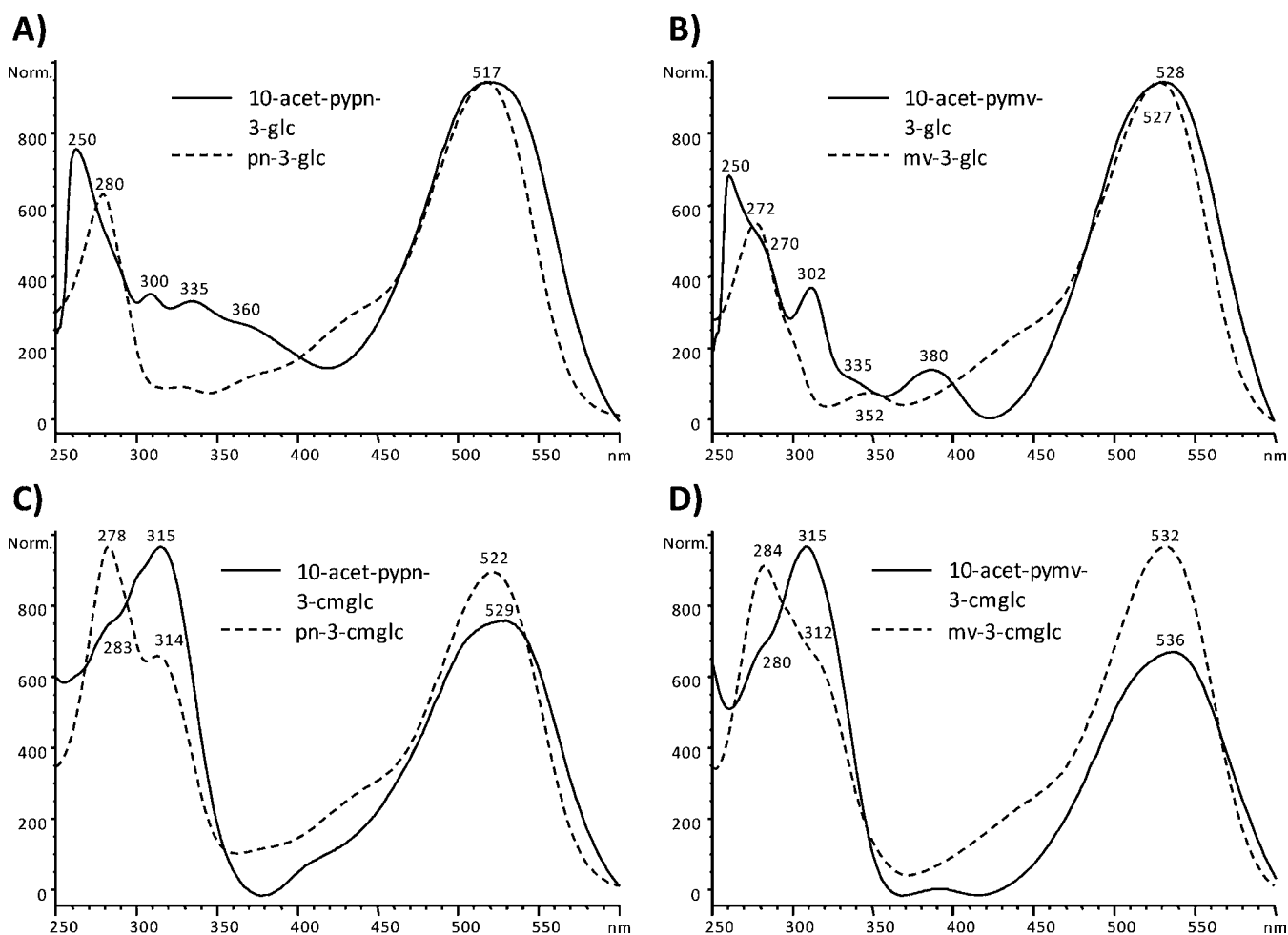


**Figure 2.** HPLC online DAD UV-vis spectra of 10-acetyl-pyranoanthocyanins and their respective anthocyanin precursors. Abbreviations: pn, peonidin; mv, malvidin; 3-glc, 3-glucoside; 3-cmglc, 3-(6'-*p*-coumaroyl)-glucoside; pypn, pyranopeonidin; and pymv, pyranomalvidin.

detected at both 520 and 280 nm), the calculated reaction yields for 10-acetyl-pyranopeonidin-3-glucoside (10-acet-pypn-3-glc) and 10-acetyl-pyranomalvidin-3-glucoside (10-acet-pymv-3-glc) were 32 and 35%, respectively; in contrast, the estimated yields for their *p*-coumaroylated derivatives, 10-acet-pypn-3-cmglc and 10-acet-pymv-3-cmglc, were higher (50 and 63%, respectively), thus suggesting that the presence of *p*-coumaroyl residue could facilitate the reaction or even stabilize the new pigments formed. Likely explanations for the aforementioned low reaction yields comprised the well-known thermal degradation of anthocyanins and also the involvement of formed 10-acetyl-pyranoanthocyanins in further reactions similar to those reported for other vitisin-like pyranoanthocyanins.<sup>3–10</sup>

The fractionation of the reaction mixture by countercurrent chromatography (FCPC) allowed the separation of almost pure 10-acet-pymv-3-glc that further was highly purified by semipreparative HPLC. However, in the case of 10-acet-pypn-3-glc, FCPC did not allow a proper fractionation, but semipreparative HPLC overcame this trouble, and also, highly pure compound was obtained. Unfortunately, we had no success in obtaining any fraction enough enriched in the *p*-coumaroylated derivatives of 10-acetyl-pyranoanthocyanins.

**Structure Elucidation of 10-Acetyl-pyranopeonidin-3-glucoside and 10-Acetyl-pyranomalvidin-3-glucoside.** The online UV-vis spectra registered for the new 10-acetyl-

pyranoanthocyanins showed remarkable differences with regard to other previously described structure-related pyranoanthocyanins bearing a nonphenolic substituent at position C-10 (the so-called vitisin-type pyranoanthocyanins). For instance, 10-carboxy-pyranoanthocyanins (also known as A-type vitisins) show well-defined visible absorbance maxima around 505–509 and 511–514 nm for compounds derived from pn-3-glc and mv-3-glc, respectively, and the analogue 10-methyl-pyranoanthocyanins have visible absorbance maxima at even lower wavelength values, around 475–480 and 480–482 nm.<sup>18</sup> For most described pyranoanthocyanins, the visible absorbance maxima are hypsochromically shifted with regard to their anthocyanin precursors, and their color is described as red-orange. However, the synthesized 10-acetyl-pyranoanthocyanins showed a broad absorbance band with not well-defined absorbance maxima at similar wavelength values with regard to their anthocyanin precursors (Figure 2). For nonacylated 10-acetyl-pyranoanthocyanins, a broad absorbance band was observed at 505–522 nm for 10-acet-pypn-3-glc (Figure 2A) and 515–532 nm for 10-acet-pymv-3-glc (Figure 2B), with the visible absorbance maxima located at the same wavelength values than their respective anthocyanin precursors. Similar results were found for *p*-coumaroylated 10-acetyl-pyranoanthocyanins, with respective broad visible absorbance bands in the ranges 510–530 (Figure 2C) and 520–542 nm (Figure 2D) and maxima even slightly bathochromically shifted with regard

to their respective anthocyanin precursors. In addition, these *p*-coumaroylated derivatives showed the expected absorbance band at 315 nm attributable to the *p*-coumaroyl residue that was the most intense band.

Mass spectrometry data were in agreement with the suggested structures of 10-acetyl-pyranoanthocyanins (Figure S1 in the Supporting Information). The MS spectra in positive ionization mode showed the expected *m/z* signals attributable to the molecular ions of the flavylum cation form in which these compounds predominantly might exist in the acidic medium used for their elution. Moreover, the MS/MS spectra (positive ionization mode) showed the expected fragmentation pattern common to pyranoanthocyanins and anthocyanins, namely, the breaking of the glucosidic bond at C-3 with a neutral loss of glucose (fragment loss of 162 amu) for nonacylated glucosides and a neutral loss of the entire 6''-*p*-coumaroyl-glucose residue (fragment loss of 308 amu), without intermediate fragmentation of the ester bond, in the case of *p*-coumaroylated glucosides.<sup>18</sup> In both cases, the resulting MS/MS fragment ions appeared at the expected *m/z* values of the aglycons 10-acetyl-pyranopeonidin (*m/z* of 367) and 10-acetyl-pyranomalvidin (*m/z* of 397).

Definitive evidence supporting the expected structures of 10-acetyl-pyranoanthocyanins was provided by the NMR spectra obtained for the two nonacylated main reaction products that could be isolated in enough amount, 10-acet-pypn-3-glc (Table 1) and 10-acet-pymv-3-glc (Table 2). The NMR spectra were registered in acidic medium to promote the almost quantitative predominance of the flavylum cation form. The obtained NMR data were in concordance with reported data for structurally related compounds, as the 10-carboxy-pyranoanthocyanins.<sup>12,24</sup> The evidence of formation of the new pyrano D ring was supported by the absence of any signal attributable to H-4, which was present in the anthocyanin precursors. In addition, a new signal appeared at 7.90–7.97 ppm having an integral value corresponding to 1 proton, which was not coupled with any other proton; this new signal was assigned to H-9 of the new D ring. The recording of the <sup>1</sup>H NMR spectrum of 10-acet-pymv-3-glc in CF<sub>3</sub>COOD–DMSO-*d*<sub>6</sub> (20:80) after 15 h of storage at 25 °C gave additional supporting evidence to the suggested structure of pyranoanthocyanin (Figure S2 in the Supporting Information). A decrease in the intensity of the signal attributable to H-9 of the new formed D ring was observed after this time. Hydrogen–deuterium (H-D) exchange in CD<sub>3</sub>OD has been reported for anthocyanin positions H-6 and H-8, whereas for A-type vitisins (10-carboxy-pyranoanthocyanins), the latter positions do not exchange, but the position H-9 does,<sup>25</sup> with a half-life for the H-D exchange of 25 h in the latter case. For 10-acet-pymv-3-glc, the signal intensity for H-9 decreased by 71% of its initial value after 15 h, thus suggesting that H-D exchange in this type of pyranoanthocyanins is faster than those described for A-type vitisins. Moreover, the signal at 2.64–2.65 ppm was not coupled with any other signal and integrated for three protons, thus being compatible to the expected acetyl group at C-10 position of the new D ring. The integral value of signals attributable to methoxy groups, together with chemical shifts and signal multiplicity (proton–proton coupling constants) assigned to protons of the B ring, allowed the confirmation of the corresponding peonidin and malvidin substitution patterns. Finally, the chemical shifts and, especially, the proton–proton coupling constants values attributable to the glucosidic moiety were compatible, in both cases, with a glucose linked in the β anomeric configuration to

**Table 1.** NMR Spectroscopic Data Registered in CD<sub>3</sub>OD–CF<sub>3</sub>COOD (70:30, v/v) for 10-Acetyl-pyranopeonidin-3-*O*-β-glucoside: <sup>1</sup>H Data (Chemical Shifts in ppm and Coupling Constants in Hz), <sup>13</sup>C Data (Chemical Shifts in ppm), and <sup>1</sup>H–<sup>13</sup>C Correlation Experiments at One Bond (HMQC) and More Than One Bond (HMBC)

position	δ <sup>1</sup> H (J <sub>HH</sub> )	δ <sup>13</sup> C	HMQC	HMBC
C ring				
2		164.84		H-2'
3		135.14		H-9, H-1''
4		ND <sup>a</sup>		
A ring				
4a		109.60		H-6, H-8
5		152.70		H-6
6	7.16 (2.0)	100.60	H-6	
7		168.75		H-6, H-8
8	7.23 (2.1)	100.91	H-8	
8a		153.16		H-8
B ring				
1'		120.00		H-5'
2'	7.95 (2.3)	113.20	H-2'	
3'		147.76		H-5', H-2', OCH <sub>3</sub>
4'		154.20		H-2', H-6'
5'	6.99 (8.4)	115.46	H-5'	
6'	8.01 (8.6, 2.2)	126.84	H-6'	
OCH <sub>3</sub>	3.97	55.60	OCH <sub>3</sub>	
D ring				
9	7.92	103.61	H-9	
10		157.40		H-9
10-acetyl				
11 (C=O)		191.00		H-12
12 (CH <sub>3</sub> )	2.64	24.72	H-12	
3-glucoside				
1''	4.69 (7.7)	104.69	H-1''	
2''	3.67 (9.2, 8.1)	74.14	H-2''	
3''	3.39 (9.2)	76.30	H-3''	
4''	3.33 (9.5)	70.04	H-4''	
5''	3.14 (8.5, 6.1, 2.2)	77.33	H-5''	
6''A	3.66 (11.7, 2.6)	61.10	H-6''A, H-6''B	
6''B	3.42 (12.1, 6.2)			

<sup>a</sup>ND, nondetected NMR signal.

the pyranoanthocyanidin residue. The linkage position of glucose to pyranoanthocyanidin was confirmed by the detection of the corresponding long-distance <sup>1</sup>H–<sup>13</sup>C correlation (HMBC experiment) between the anomeric proton (H-1'') and the carbon at position 3 in C ring. In summary, the two main reaction products formed from the reaction of pn-3-glc and mv-3-glc with diacetyl were 10-acetyl-pyranopeonidin-3-*O*-β-glucoside (Figure 3A) and 10-acetyl-pyranomalvidin-3-*O*-β-glucoside (Figure 3B), respectively.

**NMR Study of the Different Equilibrium Forms of 10-Acetyl-pyranoanthocyanins in Solution.** It is well established that both anthocyanins and pyranoanthocyanins are involved in several equilibria in solution. In fact, the use of NMR spectroscopy for structure elucidation of pyranoanthocyanins works easier if only one of all possible forms are present in solution at the moment of spectroscopic analysis. As usual in

**Table 2.** NMR Spectroscopic Data Registered in (A) DMSO- $d_6$ -CF<sub>3</sub>COOD (80:20) and (B) CD<sub>3</sub>OD-CF<sub>3</sub>COOD (70:30) for 10-Acetyl-pyranomalvidin-3-*O*- $\beta$ -glucoside: <sup>1</sup>H Data (Chemical Shifts in ppm and Coupling Constants in Hz), <sup>13</sup>C Data (Chemical Shifts in ppm), and <sup>1</sup>H-<sup>13</sup>C Correlation Experiments at One Bond (HMQC) and More Than One Bond (HMBC)

position	$\delta$ <sup>1</sup> H ( $J_{HH}$ )		$\delta$ <sup>13</sup> C (B)	HMQC	HMBC
	A	B			
C ring					
2			164.26		H-2', H-6'
3			135.15		H-9, H-1''
4			109.60		H-9
A ring					
4a			109.40		H-8
5			152.66		H-6
6	7.32 (1.8)	7.17 (1.8)	100.66	H-6	
7			168.79		H-6, H-8
8	7.51 (1.8)	7.26 (1.8)	101.00	H-8	
8a			153.08		H-8
B ring					
1'			118.80		H-2', H-6'
2'	7.85	7.68	108.64	H-2'	
3'			148.15		H-2', H-6', OCH <sub>3</sub>
4'			143.45		H-2', H-6'
5'			148.15		H-2', H-6', OCH <sub>3</sub>
6'	7.85	7.68	108.64	H-6'	
OCH <sub>3</sub>	3.92	3.95	55.91	OCH <sub>3</sub>	
D ring					
9	7.97	7.90	103.35	H-9	
10			157.53		H-9
10-acetyl					
11 (C=O)			191.00		H-12
12 (CH <sub>3</sub> )	2.65	2.65	24.75	H-12	
3-glucoside					
1''	4.75 (7.8)	4.69 (7.8)	104.29	H-1''	
2''	3.48 (9.2, 7.8)	3.68 (9.2, 7.8)	74.25	H-2''	
3''	3.22 (9.2, 8.8)	3.44 (9.2, 8.8)	76.43	H-3''	
4''	3.15 m	3.41 m	70.03	H-4''	
5''	3.02 (9.0, 7.0, 1.9)	3.14 (9.0, 7.0, 1.9)	77.48	H-5''	
6''A	3.44 (11.5, 1.9)	3.67 (11.5, 1.9)	61.21	H-6''A, H-6''B	
6''B	3.28 (11.5, 7.0)	3.46 (11.5, 7.0)			

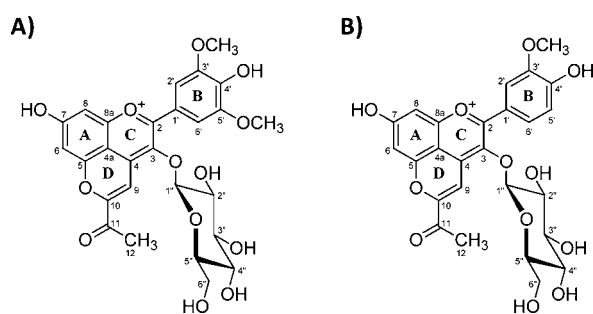


**Figure 3.** Chemical structures of synthesized and isolated 10-acetyl-pyranomalvidin-3-*O*- $\beta$ -glucoside (A) and 10-acetyl-pyranopeonidin-3-*O*- $\beta$ -glucoside (B) in their flavylium cation forms.

the NMR analysis of these compounds, a strong acidic medium (trifluoroacetic acid in proportions 2–10%), mainly in nonaqueous solvents (DMSO- $d_6$  or CD<sub>3</sub>OD), allows that only the flavylium cation form was occurring, and subsequently, most of reported NMR data for anthocyanins and pyranoanthocyanins are those of their flavylium cation forms.

However, the recording of NMR spectra of the isolated 10-acetyl-pyranoanthocyanins using up to 10% CF<sub>3</sub>COOD in both

CD<sub>3</sub>OD and DMSO- $d_6$  always resulted in a mixture of the expected signals attributable to the flavylium cation form together with two sets of signals occurring in similar proportions (Figure 4A), which were tentatively assigned to neutral hemiacetal forms. The mixture of different forms in equilibrium was quite evident with regard to the signal attributable to the anomeric proton (H-1'') of the glucose residue, which appeared as a set of three signals (three doublets with identical constant coupling): the most intense was assigned to the flavylium cation form, whereas the other two of similar intensity were assigned to the two possible epimeric isomers of the resulting hemiacetal forms following hydration of flavylium cation form.<sup>26</sup> One proof supporting that we were dealing with a mixture of different forms in equilibrium was given by the increase of the anomeric proton signal of flavylium cation form (H-1'' f) and the parallel decrease of both signals of epimeric hemiacetal forms (H-1'' hm-a and hm-b) when the percentage of CF<sub>3</sub>COOD was increased (Figure 4C). The set of signals attributable to hemiacetal forms was still present as traces in the NMR spectrum recorded in CF<sub>3</sub>COOD-CD<sub>3</sub>OD (30:70), but they totally disappeared using CF<sub>3</sub>COOD-DMSO- $d_6$  (20:80) (Figure 4B). Unfortunately, the use of CF<sub>3</sub>COOD-DMSO- $d_6$  (20:80) resulted in some extent of hydrolysis of the glucosidic

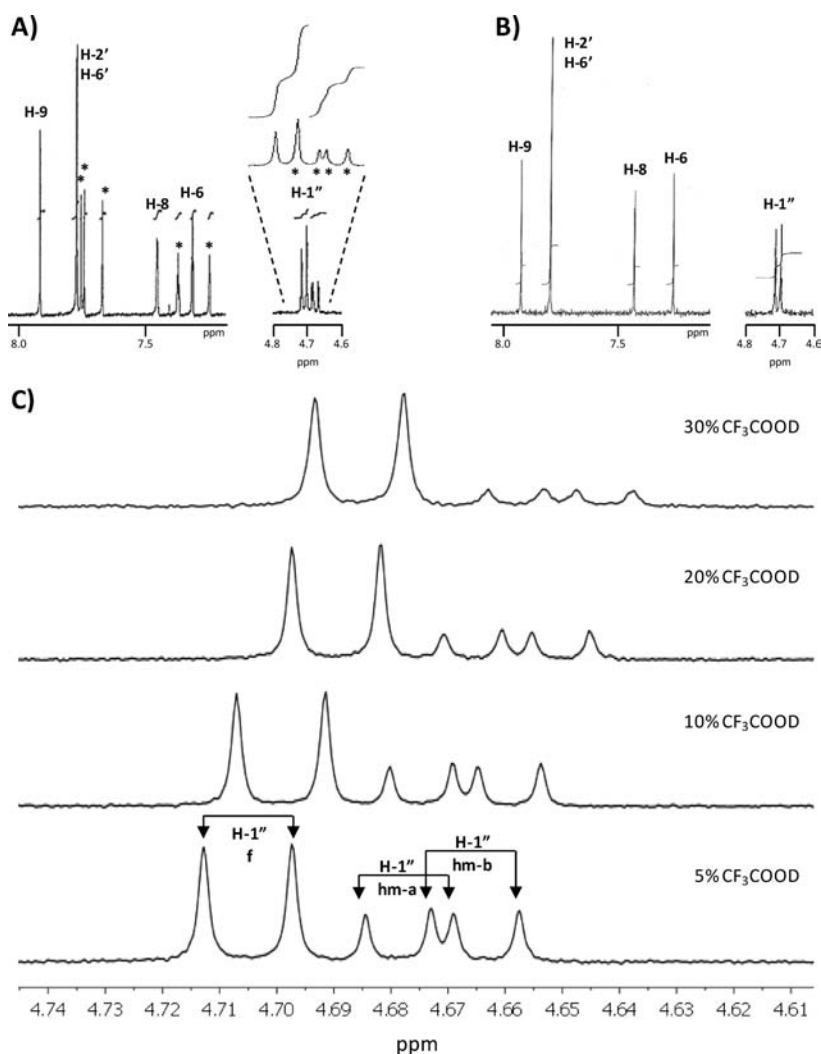


**Figure 4.**  $^1\text{H}$  NMR signals corresponding to the anomeric ( $\text{H-1}''$ ) and aromatic protons in rings A ( $\text{H-6}$  and  $\text{H-8}$ ), B ( $\text{H-2}'$  and  $\text{H-6}'$ ), and D ( $\text{H-9}$ ) for spectra of 10-acetyl-pyranoanthocyanins registered in different solvents: (A) 10-acet-pymv-3-glc in  $\text{CD}_3\text{OD}$  with 2%  $\text{CF}_3\text{COOD}$  (asterisks indicate signals assigned to hemiacetal forms), (B) 10-acet-pymv-3-glc in  $\text{DMSO-}d_6$  with 20%  $\text{CF}_3\text{COOD}$ , and (C) anomeric proton ( $\text{H-1}''$ ) section of 10-acet-pypn-3-glc spectra in  $\text{CD}_3\text{OD}$  with variable proportions (5–30%) of  $\text{CF}_3\text{COOD}$ . Abbreviations: f, flavylium cation form; and hm, hemiacetal form.

bond after several hours (Figure S2 in the Supporting Information), as confirmed by chromatographic analysis, thus making unable the use of this solvent for recording of low sensitive, time-consuming,  $^{13}\text{C}$  NMR spectra. Additional evidence supporting the existence of the aforementioned suggested that equilibrium was achieved by 2D NOESY NMR experiment performed with 10-acet-pypn-3-glc in  $\text{CF}_3\text{COOD-CD}_3\text{OD}$  (5:95). Besides negative NOE cross-peaks, we observed additional positive cross-peaks that are caused by chemical exchange between the two hemiacetal forms and the same flavylium cation form of 10-acetyl-pyranoanthocyanins.<sup>26</sup> Because of the similar values of chemical shifts attributable to the anomeric proton signals for both flavylium and hemiacetal forms (Figure 4C), it was not possible to clearly observe the expected cross-peaks because they were almost indistinguishable from the correlation diagonal. Fortunately, clear positive cross-peaks could be detected for the signals assigned to the different forms of 10-acetyl protons (Table 3, 2.71 ppm for flavylium form and 1.76 and 1.74 for hemiacetal forms). As also found for anthocyanins,<sup>26</sup> the chemical

exchange was not observed between the two epimeric hemiacetal forms.

The sample of 10-acet-pymv-3-glc used for registration of NMR spectra in  $\text{CD}_3\text{OD}$  with increasing proportions of  $\text{CF}_3\text{COOD}$  showed a new chromatographic peak, eluting 5.92 min later, following several hours of storage after the recording of NMR spectra (Figure 5). However, in this case, the characteristics of the UV-vis spectrum (shape and value of maximum absorbance wavelength) were closer to those described for A- and B-type vitisins and 10-methyl-pymv-3-glc,<sup>18</sup> showing a maximum at 498 nm. In addition, this peak disappeared after drying of the sample and redissolution in 0.1 N HCl in methanol. The MS spectra of this new compound showed a similar fragmentation pattern than 10-acet-pymv-3-glc, but all signals were increased in 46 amu: molecular ion at  $m/z$  605 that originated a fragment ion at  $m/z$  443 after loss of a neutral glucose residue (162 amu). These results suggested that the newly formed compound was likely the product of the addition of two molecules of methanol to the carbonyl of the 10-acetyl substituent of 10-acet-pymv-3-glc; that is, the new compound should be 10-(1',1'-dimethoxy)-ethyl-pymv-3-glc.

**Table 3. Chemical Shifts of Nuclei ( $^1\text{H}$  and  $^{13}\text{C}$ ) Showing the Greatest Differences with Regard to Compound 10-Acetylpyranomalvidin-3-*O*- $\beta$ -glucoside Were in the Flavylium Cation (f) or Epimeric Hemiacetal (hm-a and hm-b) Forms<sup>a</sup>**

position	f form	hm-a form	hm-b form
$^1\text{H}$ nuclei			
H-9	7.88	7.61	7.61
H-1''	4.71	4.67	4.68
CH <sub>3</sub>	2.71	1.76	1.74
H-2',6'	7.72	7.69	7.70
$^{13}\text{C}$ nuclei			
CH <sub>3</sub>	24.7	25.2	25.4
C=O	190.8	171.9	171.9
C-10	157.5	97.0	97.0
C-4	111.0	108.3	108.3
C-3	135.2	133.9	133.9
C-2	164.3	164.0	164.0
C-1'	118.8	118.0	118.0
C-3',5'	148.2	148.9	148.9
C-4'	143.5	143.6	143.6

<sup>a</sup>Spectrum registered in CD<sub>3</sub>OD–CF<sub>3</sub>COOD (98:2).

This kind of derivative was also observed when 10-acet-pypn-3-glc was kept in methanolic solution with 30% CF<sub>3</sub>COOH for 48 h at room temperature. A minor new chromatographic peak appeared eluting 5.93 min later, showing a visible absorbance maximum at 491 nm and having a molecular ion at *m/z* 575 that further fragmented resulting in a product ion at *m/z* 413 (again the same *m/z* values for molecular and fragment ions than 10-acet-pypn-3-glc, but both increased in 46 amu). The formation of these dimethoxy derivatives suggested the high reactivity of the carbonyl of the 10-acetyl substituent of 10-acetyl-pyranoanthocyanins. This question will be discussed later with regard to the results of stability of these pigments toward SO<sub>2</sub> bleaching.

Looking back to the suggested occurrence of hemiacetal forms of 10-acetyl-pyranoanthocyanins detected in the  $^1\text{H}$  NMR spectra of these compounds, it is necessary to remark that two possible positions are available for hydration of the flavylium cation form, namely, positions C-2 and C-10 (Figure S3 in the Supporting Information). Previous studies have demonstrated that the presence of new D ring in pyranoanthocyanins increases their stability toward nucleophilic attack of water (resulting in the formation of hemiacetal forms) or bisulfite ion, both resulting in color loss (bleaching), in

comparison to their anthocyanin precursors.<sup>27–29</sup> Moreover, several studies had reported that pyranoanthocyanins were only involved in proton transfer equilibria, and the formation of hemiacetal forms had been not observed.<sup>14,15</sup> However, vitisin A has been suggested to form the hemiacetal forms at both C-2 and C-10 position;<sup>13</sup> more recently, a study reported that 10-methyl-pyranomalvidin-3-glucoside in weak acidic (pH 5) aqueous medium could give rise to a minor hemiacetal form together with the flavylium cation and neutral quinoidal base forms, but the position of nucleophilic addition was not specified.<sup>17</sup>

An in-depth analysis of NMR spectra of 10-acet-pymv-3-glc in CD<sub>3</sub>OD–CF<sub>3</sub>COOD (98:2) (the less acidic medium assayed, thus favoring the formation of hemiacetal forms) provided enough evidence to suggest that the hemiacetal forms were formed by nucleophilic attack of water to C-10, thus originating a mixture of two epimeric isomers in similar proportions. The key was to determine whether, as a result of hemiacetal formation, the chemical shift of the possibly involved carbon (C-2 or C-10) was affected. NMR studies dealing with anthocyanins have determined that hemiacetal formation is located in C-2, because an upfield shift (lower value of chemical shift) of 61 ppm was observed for this nucleus as compared to its anthocyanin precursor.<sup>26</sup> The long-distance  $^1\text{H}$ – $^{13}\text{C}$  correlation experiments (HMBC; Figure S4 in the Supporting Information) allowed us to determine the chemical shifts of the nuclei involved in the possible location of hydration position for both the flavylium cation and the two epimeric hemiacetal forms (Table 3). Chemical shift values of carbon nuclei of B ring (C-1'; C-3' and 5'; C-4') and C-2 assigned to hemiacetal forms differed little with regard to those corresponding to flavylium cation form. However, the chemical shift of C-10 assigned to hemiacetal forms was upfield shifted by 60.5 ppm with regard to the value for its flavylium cation form. In addition, other nuclei showed lower upfield shifts (carbonyl carbon of acetyl group) or even did not change their chemical shift values in their hemiacetal forms as compared to their corresponding flavylium cation form. The aforementioned results strongly evidenced that hydration position of 10-acetyl-pyranoanthocyanins is located at C-10.

**Color Properties of 10-Acetyl-pyranopeonidin-3-glucoside and 10-Acetyl-pyranomalvidin-3-glucoside.** Anthocyanins are unstable compounds involved in several acidic–basic equilibria in aqueous solution and also suffer nucleophilic attack to positions C-2 and C-4 of its flavylium cation form.<sup>30</sup>

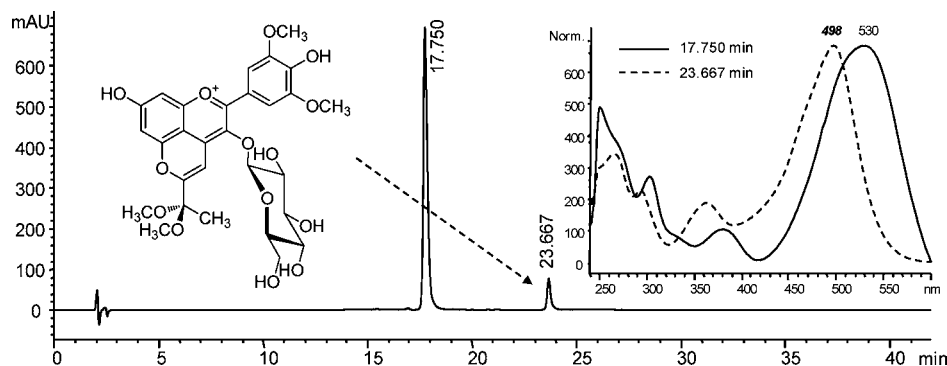


**Figure 5.** Chromatogram (detection at 520 nm) corresponding to the sample of 10-acet-pymv-3-glc just after recording the  $^1\text{H}$  NMR in CD<sub>3</sub>OD with 30% of CF<sub>3</sub>COOD. The online UV–vis spectra of 10-acet-pymv-3-glc (17.750 min) and the newly formed compound (23.667 min) is also shown, as well as the suggested chemical structure of 10-(1',1'-dimethoxy)-ethyl-pymv-3-glc for the latter.

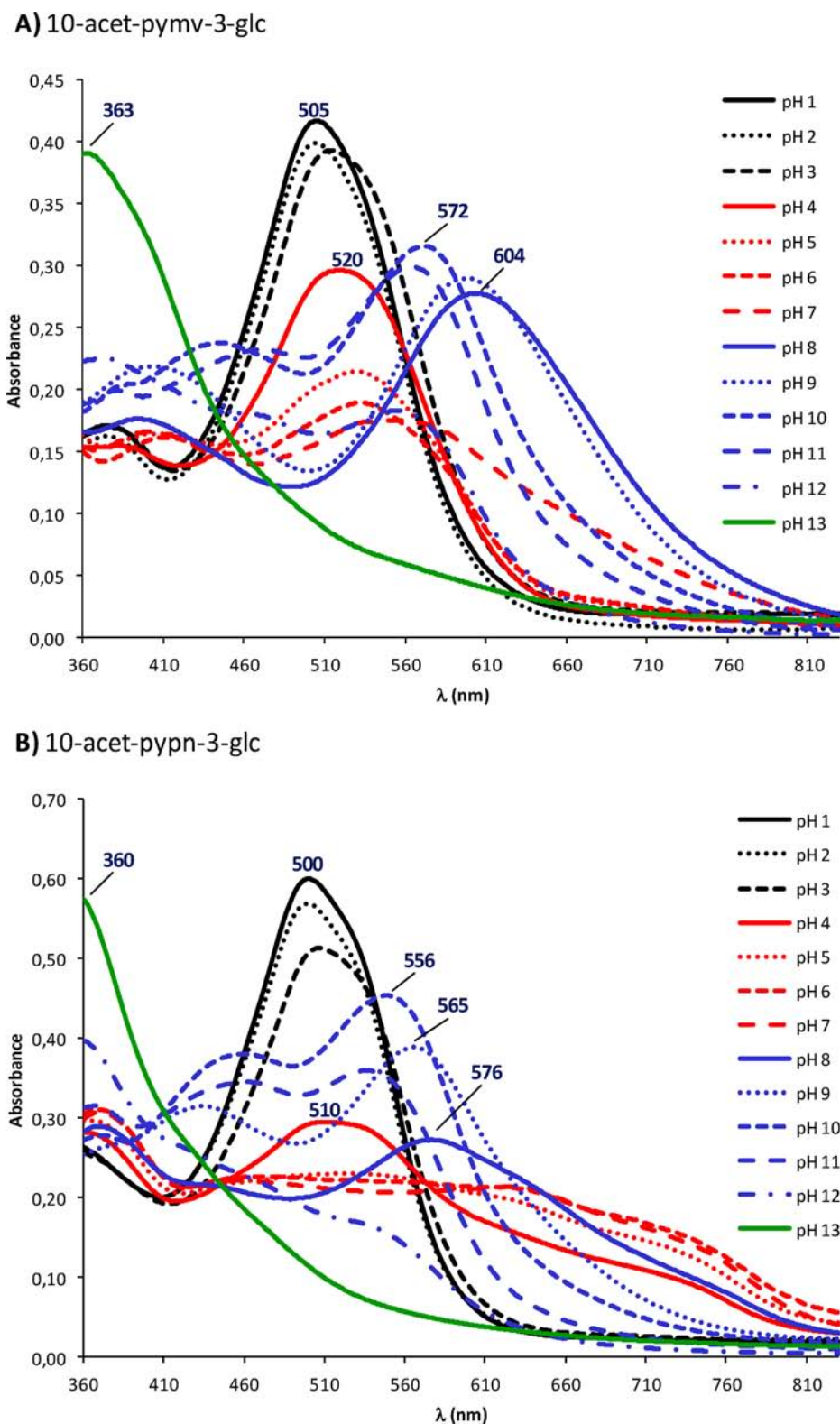


**Figure 6.** Changes in the visible spectra of 10-acetyl-pyranoanthocyanins as a function of pH: (A) 10-acet-pymv-3-glc and (B) 10-acet-pypn-3-glc.

With regard to acidic–basic equilibria, the red-colored flavylium cation form predominates in strong acidic medium. As the pH increases, this cationic form loses protons to form, successively, the blue-colored neutral and anionic quinoidal bases. Pyranoanthocyanins are also involved in those aforementioned acidic–basic equilibria.<sup>5,11–17</sup> With regard to nucleophilic attack, position C-2 is the preferred for water as

nucleophilic agent, whereas C-4 is the only available position for bisulfite because the steric hindrance of position C-2.<sup>31</sup> In both cases, the formed adduct breaks the aromaticity of C ring, and the resulting compound is colorless (bleaching effect). The ability of bisulfite bleaching is apparently lost by pyranoanthocyanins because the position C-4 is involved in the formation of the new D ring and is not available for nucleophilic attack.

Moreover, the nucleophilic attack of water to position C-2 of pyranoanthocyanins is notably decreased. For those reasons, pyranoanthocyanins are described as more stable pigments with regard to their anthocyanin precursors, and it is usual to evaluate how much more stable they are.

The visible spectra of 10-acetyl-pyranoanthocyanins were modified when registered in aqueous solution in a pH range 1–13 (Figure 6) as it also has been reported for analogous compounds like vitisin A.<sup>13</sup> At strong acidic media (pH < 4.0), the absorbance maxima were in the range 500–505 nm, with the highest value corresponding to pyranomalvidin derivative, in agreement to previous findings related to the B ring substitution pattern of vitisin-type pyranoanthocyanins.<sup>18</sup> At those very acidic pH values, the flavylium cation form must predominate, but a broadening of the visible absorbance band, together with a bathochromic shift and a parallel decrease in the absorbance maximum intensity, was observed following pH increase.

At pH around 4.0, the visible spectra showed a broad absorbance band with maximum around 510–520 nm. This behavior could be likely explained as the result of two concurrent processes. On one hand, the formation of hemiacetal forms (colorless form) cause a decrease in red color intensity as evidenced the NMR data. On the other hand, the beginning of the deprotonation of the flavylium cation form to give rise to the neutral quinoidal base (blue-colored form), which was increasing its proportion as the pH value increased up to reach a purple-blue color in weak basic media (around 8.0–9.0), with an absorbance maximum at 604 nm for 10-acet-pymv-3-glc (Figure 6A) and 576 nm for 10-acet-pypn-3-glc (Figure 6B).

At strong basic conditions (pH 10.0–12.0), the neutral quinoidal bases should be subsequently deprotonated to form the anionic quinoidal base, and this process was accompanied by a hypsochromic shift of the visible absorbance maximum, at around 560 nm. Finally, at pH 13.0, the visible absorbance maximum changed to 360 nm, and the solution was light yellow.

The above-mentioned results suggest that at usual red wine pH values (3.5–4.0), the 10-acetyl-pyranoanthocyanins do not exist exclusively as flavylium cation forms, the contributions of hemiacetal and neutral quinoidal base forms being remarkable. A similar behavior has been reported for the analogous pyranoanthocyanin called vitisin A (10-carboxy-pyranomalvidin-3-glucoside) that at wine pH (3.2–3.8) is in a complex mixture of neutral and anionic, hydrated, and nonhydrated states, where the principal species was the orange quinoidal base.<sup>13</sup> Thus, the calculation of molar extinction coefficients of 10-acetyl-pyranoanthocyanins suggested that these pigments show similar color hue and intensity than their anthocyanin precursors in real wine conditions (Table 4). 10-Acetyl-

**Table 4. Molar Extinction Coefficient at Different pH Values for Reference Wavelength (520 nm) and for Absorbance Maximum Wavelength Corresponding to Each Pigment and pH Value**

pigment	pH 1.0			pH 3.6		
	$\epsilon_{520}$	$\lambda_{\max}$	$\epsilon_{\max}$	$\epsilon_{520}$	$\lambda_{\max}$	$\epsilon_{\max}$
mv-3-glc	28100	520	28100	10600	526	10800
10-acet-pymv-3-glc	9700	507	10200	7800	515	7900
10-acet-pypn-3-glc	7000	499	7600	4700	508	4800

pyranoanthocyanins are red pigments with lower coloration capacity than anthocyanins at strong acid media (pH 1.0), showing a molar extinction coefficient at 520 nm of 9700 for 10-acet-pymv-3-glc versus 28100, the value obtained for mv-3-glc, which is also in agreement with literature data.<sup>11</sup> However, at red wine pH conditions (reference pH value of 3.6), both kinds of pigment showed quite similar coloration capacity (molar extinction coefficients of 7800 and 10600, respectively), but the decrease in coloration capacity suffered by mv-3-glc (from pH 1.0 to 3.6) was higher than that of 10-acet-pymv-3-glc (62 and 20%, respectively; 34% in the case of 10-acet-pypn-3-glc). This decrease is likely because of the formation of hemiacetal forms, but 10-acetyl-pyranoanthocyanins were more resistant to this process than their anthocyanin precursors. Moreover, the CIELAB color parameters calculated at pH 3.6 are a reflection of the aforementioned results (Table 5): at

**Table 5. CIELAB Color Parameters Measured at pH 3.6 for 0.08 mM Pigment Solutions**

pigment	$L^*$	$a^*$	$b^*$	$C^*$	$h^*$
mv-3-glc	70.56	54.74	-6.42	55.12	353.31
10-acet-pymv-3-glc	70.10	40.70	-5.88	41.12	351.78
10-acet-pypn-3-glc	78.70	26.86	-0.29	26.86	359.39

equal molar concentrations, 10-acet-pymv-3-glc shows color characteristics very close to those of mv-3-glc, the only difference being a slight lower contribution of the red component ( $a^*$ ) of the former pigment with parallel lower chroma value ( $C^*$ ). Finally, the B ring substitution pattern affected the color characteristics of 10-acetyl-pyranoanthocyanins, as also found for anthocyanins and other vitisin-type pyranoanthocyanins:<sup>18</sup> on one hand, a bathochromic shift of 8 nm is observed in B ring trisubstituted compounds (10-acet-pymv-3-glc) with regard to disubstituted ones (10-acet-pypn-3-glc), which is independent of the pH value; on the other hand, the molar extinction coefficient was notably higher for trisubstituted compounds (35% more at pH 1.0; 65% more at pH 3.6). These differences also reflected on the CIELAB color parameters shown by 10-acet-pypn-3-glc with regard to 10-acet-pymv-3-glc measured at the same concentration and pH 3.6 (Table 5): its color (Figure S5 in the Supporting Information) was less intense (higher value of  $L^*$ ) with lower contributions of both red ( $a^*$ ) and blue ( $b^*$ ) color components.

The behavior of 10-acetyl-pyranoanthocyanins toward  $\text{SO}_2$  bleaching gave unexpected results as compared with previous studies dealing with other pyranoanthocyanins (Figure 7). First, the samples did not bleach after  $\text{SO}_2$  addition, and a hypsochromic shift of the color hue was observed to red-orange nuances. Moreover, the color intensity increased in parallel to concentrations of added  $\text{SO}_2$ . The wavelength of absorbance maximum after addition of  $\text{SO}_2$  (491 nm for 10-acet-pymv-3-glc and 487 nm for 10-acet-pypn-3-glc) and the shape of spectra resembled those of vitisin-type pyranoanthocyanins, especially those of 10-methyl-pyranoanthocyanins.<sup>18</sup> NMR data have supported that nucleophilic attack of water was in C-10 position of 10-acetyl-pyranoanthocyanins, but in the case of bisulfite ion (the ionic species formed by  $\text{SO}_2$  in acidic aqueous media), it is expected that steric hindrance of the acetyl group would prevent the formation of an addition compound. Moreover, if bisulfite attacks happened in C-10, a decrease in color intensity must be observed as in the case of

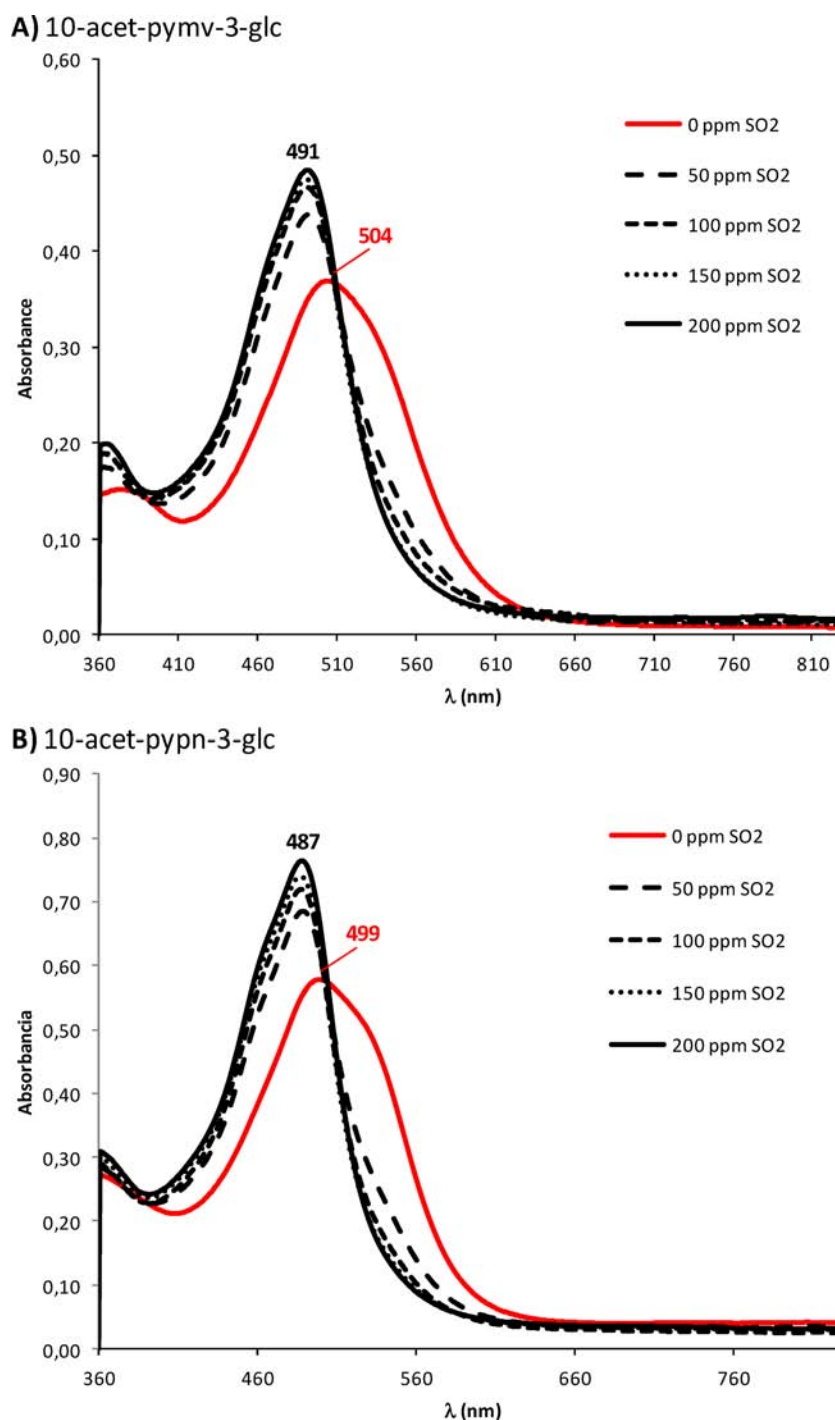


**Figure 7.** Changes in the visible spectra of 10-acetyl-pyranoanthocyanins as a function of the concentration of added SO<sub>2</sub> at pH 2.0: (A) 10-acet-pymv-3-glc and (B) 10-acet-pypn-3-glc.

the formation of hemiacetal form. Therefore, bisulfite has to attack another electrophilic position of the molecule, as the carbonyl of the 10-acetyl substituent. The resulting adduct (Figure 8A) could eliminate the conjugation of acetyl group with D ring and the new substituent at C-10 could resemble, in terms of visible absorption spectrum, the structural features of 10-methyl-pyranoanthocyanins. This result is in the same way of the finding reported in the latter section dealing with the formation of dimethoxy derivatives of 10-acetyl-pyranoanthocyanins in acidic methanolic solutions. Both results suggest a

high reactivity of the 10-acetyl group of this kind of pyranoanthocyanins.

The HPLC chromatograms of samples of 10-acetyl-pyranoanthocyanins treated with SO<sub>2</sub> did not show any additional peak attributable to the suggested adduct with bisulfite. However, direct injection of reaction mixture in the MS detector allowed the detection of the expected molecular ion for the suggested adduct (Figure 8B; a similar molecular ion at  $m/z$  611 was observed for the reaction mixture of 10-acetyl-pypn-3-glc). Moreover, the MS<sup>2</sup> spectra showed a fragment ion assignable to 10-acet-pymv-3-glc by loss of a molecule of

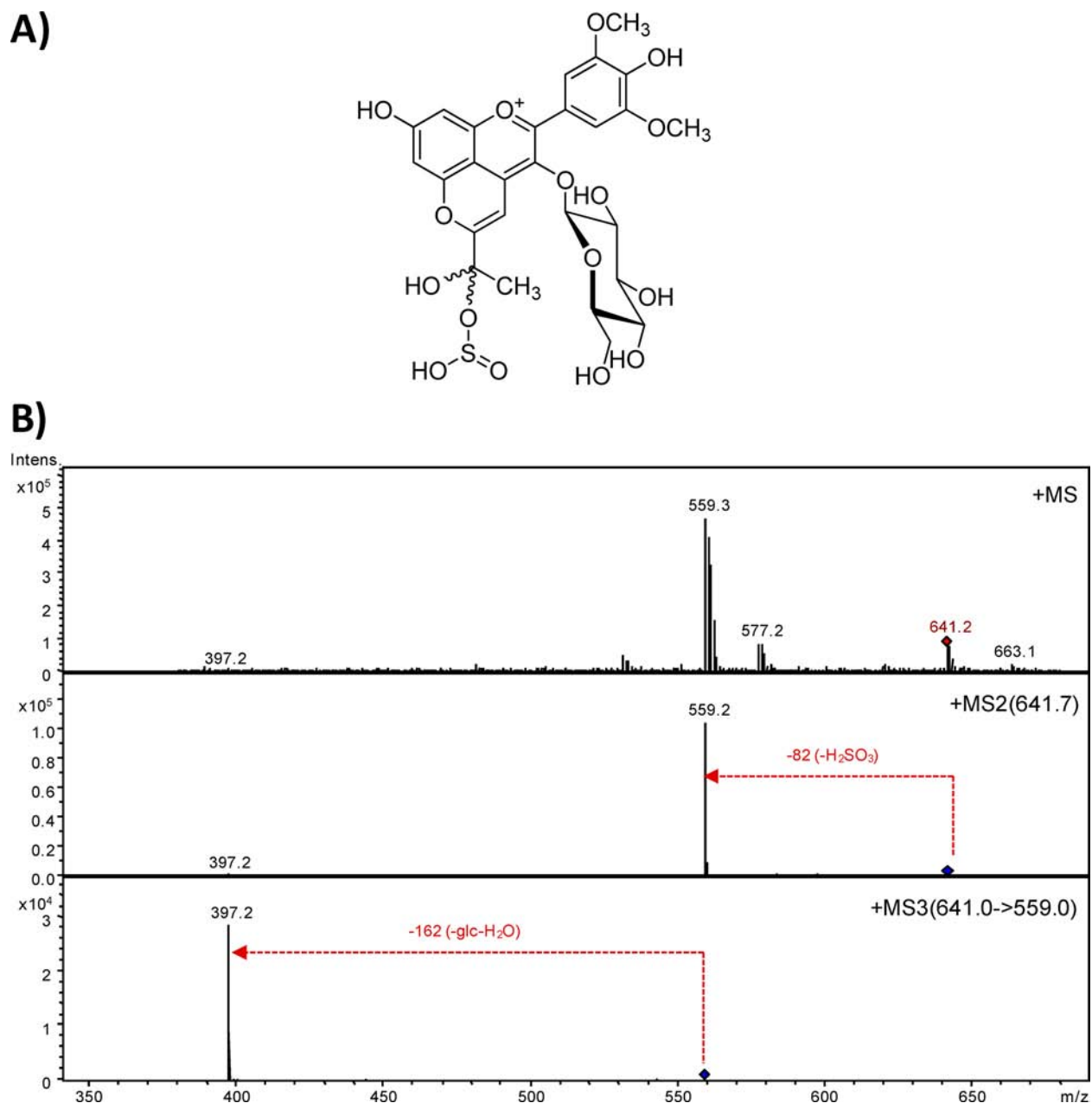


**Figure 8.** Reaction product of nucleophilic attack of  $\text{SO}_2$  to 10-acet-pymv-3-glc: (A) suggested structure and (B) mass spectra ( $\text{MS}$ ,  $\text{MS}^2$ , and  $\text{MS}^3$ ).

$\text{H}_2\text{SO}_3$ , and the  $\text{MS}^3$  spectra give rise to the subsequent aglycon 10-acet-pymv by loss of the glucose unit. A similar behavior was observed for the  $\text{MS}^2$  and  $\text{MS}^3$  spectra corresponding to the bisulfite adduct formed from 10-acet-3pypn-3-glc. The aforementioned result suggests that bisulfite adduct is very labile, and it is likely the reason why it was not observed under chromatographic conditions used.

In conclusion, this study describes the synthesis, isolation, structure elucidation, and color properties of a new type of vitisin-like pyranoanthocyanins derived from analogous grape anthocyanins and diacetyl, the so-called 10-acetyl-pyranoanthocyanins, which were previously detected in red wines. These pigments exhibit unusual properties like forming colored adducts with bisulfite. Significant proportions of these pigments seem to exist on their hemiacetal and quinoidal base equilibrium forms at weakly acidic pH. At wine pH, the color exhibited by these new pigments is described as red-purple, in

contrast to the most common red-orange color reported for other vitisin-like pyranoanthocyanins. It would be of interest further investigation about the factors influencing the formation of 10-acetyl-pyranoanthocyanins in red wine: extent of diacetyl production by microorganisms involved in alcoholic and malolactic fermentations, competing reactions of anthocyanin precursors, and their evolution after formation as suggested by both the low reaction yields observed in their synthesis and the reported reactivity for other similar vitisin-like pyranoanthocyanins.

## ■ ASSOCIATED CONTENT

### 📄 Supporting Information

Figure S1, MS and MS/MS spectra used for identification of 10-acetyl-pyranoanthocyanins; Figure S2,  $^1\text{H}$  NMR spectra of 10-acetyl-pyranomalvidin-3-glucoside in  $\text{CD}_3\text{OD}-\text{CF}_3\text{COOD}$  (80:20), fresh solution, and 15 h stored solution at room

temperature; Figure 3S, resonance forms of 10-acet-pymv-3-glc involving oxygen atoms of rings C and D and suggested formation of hemiacetals of this compound at positions C-2 and C-10; Figure S4, long-distance  $^1\text{H}$ – $^{13}\text{C}$  correlations found for the hemiacetal form of 10-acetyl-pyranomalvidin-3-glucoside; and Figure S5, color shown by aqueous solutions at pH 3.6 and concentration of 0.08 mM 10-acetyl-pyranomalvidin-3-glucoside and 10-acetyl-pyranopeonidin-3-glucoside. This material is available free of charge via the Internet at <http://pubs.acs.org>.

## AUTHOR INFORMATION

### Corresponding Author

\*Tel: ++34-926-295253. Fax: ++34-926-295351. E-mail: isidro.hermosin@uclm.es.

### Funding

S.G.-A. and M.V.G. thank the Fondo Social Europeo and Junta de Comunidades de Castilla-La Mancha for cofunding of their contracts through the INCRECYT program.

### Notes

The authors declare no competing financial interest.

## REFERENCES

(1) Monagas, M.; Bartolomé, B. Anthocyanins and anthocyanin-derived compounds. In *Wine Chemistry and Biochemistry*; Moreno-Arribas, M. V., Polo, M. C., Eds.; Springer Science and Business Media: New York, NY, 2009; pp 439–462.

(2) Rentzsch, M.; Schwarz, M.; Winterhalter, P. Pyranoanthocyanins: An overview on structures, occurrence and pathways of formation. *Trends Food Sci. Technol.* **2007**, *18*, 526–534.

(3) Mateus, N.; Silva, A. M. S.; Rivas-Gonzalo, J. C.; Santos-Buelga, C.; de Freitas, V. A new class of blue anthocyanin-derived pigments isolated from red wines. *J. Agric. Food Chem.* **2003**, *51*, 1919–1923.

(4) Mateus, N.; Oliveira, J.; Pissarra, J.; González-Paramás, A. M.; Rivas-Gonzalo, J.; Santos-Buelga, C.; Silva, A. M. S.; de Freitas, V. A new vinylpyranoanthocyanin pigment occurring in aged red wine. *Food Chem.* **2006**, *97*, 689–695.

(5) Oliveira, J.; de Freitas, V.; Silva, A. M. S.; Mateus, N. Reaction between hydroxycinnamic acids and anthocyanin-pyruvic acid adducts yielding new portisins. *J. Agric. Food Chem.* **2007**, *55*, 6349–6356.

(6) Oliveira, J.; Azevedo, J.; Silva, A. M. S.; Teixeira, N.; Cruz, L.; Mateus, N.; de Freitas, V. Pyranoanthocyanin Dimers: A New Family of Turquoise Blue Anthocyanin-Derived Pigments Found in Port Wine. *J. Agric. Food Chem.* **2010**, *58*, 5154–5159.

(7) Oliveira, J.; Mateus, N.; de Freitas, V. Synthesis of a new bluish pigment from the reaction of a methylpyranoanthocyanin with sinapaldehyde. *Tetrahedron Lett.* **2011**, *52*, 1996–2000.

(8) Oliveira, J.; Mateus, N.; Rodriguez-Borges, J. E.; Cabrita, E. J.; Silva, A. M. S.; de Freitas, V. Synthesis of a new pyranoanthocyanin dimer linked through a methyl-methine bridge. *Tetrahedron Lett.* **2011**, *52*, 2957–2960.

(9) He, J.; Oliveira, J.; Silva, A. M. S.; Mateus, N.; de Freitas, V. Oxovitisins: A New Class of Neutral Pyranone-anthocyanin Derivatives in Red Wines. *J. Agric. Food Chem.* **2010**, *58*, 8814–8819.

(10) He, J.; Silva, A. M. S.; Mateus, N.; de Freitas, V. Oxidative formation and structural characterisation of new  $\alpha$ -pyranone (lactone) compounds of non-oxonium nature originated from fruit anthocyanins. *Food Chem.* **2011**, *127*, 984–992.

(11) Håkansson, A. E.; Pardon, K.; Hayasaka, Y.; de Saa, M.; Herderich, M. Structures and colour properties of new red wine pigments. *Tetrahedron Lett.* **2003**, *44*, 4887–4891.

(12) Oliveira, J.; Fernandes, V.; Miranada, C.; Santos-Buelga, C.; Silva, A.; de Freitas, V.; Mateus, N. Color properties of four cyanidin-pyruvic acid adducts. *J. Agric. Food Chem.* **2006**, *54*, 6894–6903.

(13) Asenstorfer, R. E.; Jones, G. P. Charge equilibria and pK values of 5-carboxypyranomalvidin-3-glucoside (vitisin A) by electrophoresis and absorption spectroscopy. *Tetrahedron* **2007**, *63*, 4788–4792.

(14) Oliveira, J.; Mateus, N.; Silva, A. M. S.; de Freitas, V. Equilibrium Forms of Vitisin B Pigments in an Aqueous System Studied by NMR and Visible Spectroscopy. *J. Phys. Chem. B* **2009**, *113*, 11352–11358.

(15) Cruz, L.; Petrov, V.; Teixeira, N.; Mateus, N.; Pina, F.; de Freitas, V. Establishment of the Chemical Equilibria of Different Types of Pyranoanthocyanins in Aqueous Solutions: Evidence for the Formation of Aggregation in Pyranomalvidin-3-O-coumaroylglucoside-(+)-catechin. *J. Phys. Chem. B* **2010**, *114*, 13232–13240.

(16) He, J.; Carvalho, A. R. F.; Mateus, N.; de Freitas, V. Spectral Features and Stability of Oligomeric Pyranoanthocyanin-flavanol Pigments Isolated from Red Wines. *J. Agric. Food Chem.* **2010**, *58*, 9249–9258.

(17) Oliveira, J.; Petrov, V.; Parola, A. J.; Pina, F.; Azevedo, J.; Teixeira, N.; Brás, N. F.; Fernandes, P. A.; Mateus, N.; Ramos, F. J.; de Freitas, V. Chemical behavior of methylpyranomalvidin-3-O-glucoside in aqueous solution studied by NMR and UV-vis spectroscopy. *J. Phys. Chem. B* **2011**, *115*, 1538–1545.

(18) Blanco-Vega, D.; López-Bellido, F. J.; Alía-Robledo, J. M.; Hermosín-Gutiérrez, I. HPLC-DAD-ESI-MS/MS Characterization of Pyranoanthocyanins Pigments Formed in Model Wine. *J. Agric. Food Chem.* **2011**, *59*, 9523–9531.

(19) Castillo-Muñoz, N.; Fernández-González, M.; Gómez-Alonso, S.; García-Romero, E.; Hermosín-Gutiérrez, I. Red-Color Related Phenolic Composition of Garnacha Tintorera (*Vitis vinifera* L.) Grapes and Red Wines. *J. Agric. Food Chem.* **2009**, *57*, 7883–7891.

(20) Renault, J. H.; Thépenier, P.; Zèches-Hanrot, M.; Le Men-Olivier, L.; Durand, A.; Foucault, A.; Margraff, R. Preparative separation of anthocyanins by gradient elution centrifugal partition chromatography. *J. Chromatogr., A* **1997**, *763*, 345–352.

(21) International Organization of Vine and Wine. *HPLC-Determination of Nine Major Anthocyanins in Red and Rosé Wines*; Resolution OENO 22/2003; International Organization of Vine and Wine: Paris.

(22) Robinson, R. A.; Stokes, R. H. *Electrolyte Solutions, the Measurement and Interpretation of Conductance, Chemical Potential, and Diffusion in Solutions of Simple Electrolytes*, 2nd ed.; Butterworths: London, United Kingdom, 1968.

(23) *Determination of Chromatic Characteristics According to CIELab*; Resolution Oeno 1/2006; International Organization of Vine and Wine: Paris.

(24) Jordheim, M.; Fossen, T.; Andersen, O. M. Preparative isolation and NMR characterization of carboxypyrananthocyanins. *J. Agric. Food Chem.* **2006**, *54*, 3572–3577.

(25) Jordheim, M.; Fossen, T.; Songstadt, J.; Andersen, Ø. Reactivity of Anthocyanins and Pyranoanthocyanins. Studies on Aromatic Hydrogen–Deuterium Exchange Reactions in Methanol. *J. Agric. Food Chem.* **2007**, *55*, 8261–8268.

(26) Jordheim, M.; Fossen, T.; Andersen, Ø. Characterization of Hemiacetal Forms of Anthocyanidin 3-O- $\beta$ -Glycopyranosides. *J. Agric. Food Chem.* **2006**, *54*, 9340–9346.

(27) Sarni-Manchado, P.; Fulcrand, H.; Souquet, J. M.; Cheynier, V.; Moutounet, M. Stability and color of unreported wine anthocyanin-derived pigments. *J. Food Sci.* **1996**, *61*, 938–941.

(28) Bakker, J.; Timberlake, C. F. Isolation, identification, and characterization of new color-stable anthocyanins occurring in some red wines. *J. Agric. Food Chem.* **1997**, *45*, 35–43.

(29) Fulcrand, H.; Benabdeljalil, C.; Rigaud, J.; Cheynier, V.; Moutounet, M. A new class of wine pigments generated by reaction between pyruvic acid and grape anthocyanins. *Phytochemistry* **1998**, *47*, 1401–1407.

(30) de Freitas, V.; Mateus, N. Chemical transformations of anthocyanins yielding a variety of colours (Review). *Environ. Chem. Lett.* **2006**, *4*, 175–183.

(31) Berké, B.; Chèze, C.; Vercauteren, J.; Deffieux, G. Bisulfite addition to anthocyanins: Revisited structures of colourless adducts. *Tetrahedron Lett.* **1998**, *32*, 5771–5774.